Journal of Inorganic Biochemistry 167 (2017) 68–79

Contents lists available at ScienceDirect

Journal of Inorganic Biochemistry

journal homepage: www.elsevier.com/locate/jinorgbio

Biophysical characterization and antineoplastic activity of new bis(thiosemicarbazonato) Cu(II) complexes

Elisa Palma [a,b], Filipa Mendes [a], Goreti Ribeiro Morais [a,1], Inês Rodrigues [a], Isabel Cordeiro Santos [a], Maria Paula C. Campello [a], Paula Raposinho [a], Isabel Correia [b], Sofia Gama [a,2], Dulce Belo [a], Vítor Alves [c], Antero J. Abrunhosa [c], Isabel Santos [a], António Paulo [a,*]

[a] Centro de Ciências e Tecnologias Nucleares, Instituto Superior Técnico, Universidade de Lisboa, Estrada Nacional 10 (km 139,7), 2695-066 Bobadela LRS, Portugal
[b] Centro Química Estrutural, Instituto Superior Técnico, Universidade de Lisboa, Av. Rovisco Pais, 1049-001 Lisboa, Portugal
[c] Instituto de Ciências Nucleares Aplicadas à Saúde, Universidade de Coimbra, Coimbra, Portugal

ARTICLE INFO

Article history:
Received 1 September 2016
Received in revised form 18 November 2016
Accepted 22 November 2016
Available online 23 November 2016

Keywords:
Copper
Bis(thiosemicarbazones)
Metallodrugs
Cancer theranostics

ABSTRACT

Aiming to explore alternative mechanisms of cellular uptake and cytotoxicity, we have studied a new family of copper(II) complexes (**CuL^1-CuL^4**) with bis(thiosemicarbazone) (BTSC) ligands containing pendant protonable cyclic amines (morpholine and piperidine). Herein, we report on the synthesis and characterization of these new complexes, as well as on their biological performance (cytotoxic activity, cellular uptake, protein and DNA binding), in comparison with the parental **Cu^{II}ATSM** (ATSM = diacetyl-bis(N4-methylthiosemicarbazonate) complex without pendant cyclic amines. The new compounds have been characterized by a range of analytical techniques including ESI-MS, IR spectroscopy, cyclic voltammetry, reverse-phase HPLC and X-ray spectroscopy. In vitro cytotoxicity studies revealed that the copper complexes are cytotoxic, unlike the corresponding ligands, with a similar potency to that of **CuATSM**. Unlike **CuATSM**, the new complexes were able to circumvent cisplatin cross-resistance. The presence of the protonable cyclic amines did not lead to an enhancement of the interaction of the complexes with human serum albumin or calf thymus DNA. However, **CuL^1–CuL^4** showed a remarkably augmented cellular uptake compared with **CuATSM**, as proved by uptake, internalization and externalization studies that were performed using the radioactive congeners **^{64}CuL^1-^{64}CuL^4**. The enhanced cellular uptake of **CuL^1-CuL^4** indicates that this new family of Cu^{II}BTSC complexes deserves to be further evaluated in the design of metallodrugs for cancer theranostics.

1. Introduction

Thiosemicarbazones and their metal complexes present a wide range of applications that stretch from analytical chemistry, through pharmacology to nuclear medicine [1–5]. In the last few years there has been growing attention towards this class of compounds due to their relevant biological properties, specifically as antifungal, antiviral, antibacterial and anticancer agents [4,6–15].

In particular, it has been proved that neutral, planar and lipophilic Cu(II) bis(thiosemicarbazonato) complexes (Cu^{II}BTSC) show potential as therapeutic compounds for cancer and neurodegenerative diseases [16]. The antitumoral effect of Cu^{II}BTSC complexes is not fully understood, being attributed to several factors. These complexes are cell permeable that can act, in some cases, as redox active "copper transporters" to deposit copper within cells by binding to intracellular thiols, such as metallothioneins [16,17]. On the other hand, Cu^{II}BTSC analogues with increased lipophilicity can interact strongly with lipid bilayers, being trapped in the plasma membrane unreactive to cytosolic reductants [18,19]. Furthermore, when Cu^{II}BTSC complexes persist in their intact and unreduced forms, as a result of the proper redox properties, they can accumulate as hydrophobic aggregates in the reducing cytosolic environment [20,21]. These intact forms of Cu^{II}BTSC may exert a cellular effect, namely by inhibiting DNA synthesis, presumably by intercalation into the DNA and/or binding to DNA topoisomerases or disruption of ATP production [16,21–23].

Copper complexes of bis(thiosemicarbazones) can be readily obtained using radioactive copper under aqueous conditions, required for the synthesis and/or formulation of radiopharmaceuticals. For this reason, radioactive Cu^{II}BTSC complexes have been the subject of intense research, namely using ^{64}Cu ($t_{1/2}$ = 12.7 h), one of the most versatile radiometals in nuclear medicine. ^{64}Cu undergoes β^+ (20%) and β^- (37%) decay, emitting in addition Auger electrons with a high linear energy-transfer of 6.84 keV and a short penetration range of ≅5 μm. Due to

* Corresponding author.
E-mail address: apaulo@ctn.tecnico.ulisboa.pt (A. Paulo).
[1] Current address: Institute of Cancer Therapeutics, School of Life Sciences, University of Bradford, Bradford, UK.
[2] Current address: Institut für Anorganische und Analytische Chemie, Friedrich-Schiller-Universität Jena, Germany.

http://dx.doi.org/10.1016/j.jinorgbio.2016.11.026
0162-0134/

these unique decay characteristics, ^{64}Cu is suitable both for positron emission tomography (PET) imaging and targeted radionuclide therapy, raising the possibility of a theranostic approach [16,24–26].

So far, ^{64}Cu^{II}BTSCs have provided clinically useful results in the specific targeting of hypoxic tissue. One of the most promising radiotracers is **^{64}CuATSM** (**ATSM** = diacetyl-bis(N4-methylthiosemicarbazonate) that has been thoroughly investigated as a PET tracer for tumor hypoxia imaging [27–36]. Numerous publications describing in vitro chemical, biochemical and spectroscopic studies and in vivo results using PET imaging, allowed to conclude that the mechanism by which CuATSM-like complexes are hypoxia-selective involves intricate intracellular reduction-oxidation events, leading to an abundance of Cu(I) species.

Two mechanisms have been proposed, both related with the reduction of Cu^{II} to Cu^{I} in hypoxic conditions. The first proposed by Fujibayashi et al. [28] suggest that upon intracellular reduction in hypoxic cells, **Cu^{I}ATSM** becomes trapped irreversibly. Nevertheless, this mechanism was not fully consistent with washout studies [29], which led to the proposal of a second mechanism by the Blower group [37, 35,38]. They postulated that **CuATSM** reduction is reversible and occurs in both hypoxic and normoxic cells, generating an unstable, anionic copper(I) complex, $[Cu^{I}ATSM]^{-1}$. This species dissociates slowly in cells with low oxygen concentration leading to irreversible trapping of the Cu^{I} ion. In normoxic conditions, $[Cu^{I}ATSM]^{-1}$ may be re-oxidized by molecular oxygen to the neutral $[Cu^{II}ATSM]^{0}$ complex, which could then diffuse back out of the cell. In this mechanism, the origins of hypoxia-selective uptake and trapping may reside with the relative structure-dependent stability of the reduced Cu^{I} anion towards protonation and subsequent ligand dissociation and not only with the rate of reduction and oxidation [36,39]

Here we present a detailed study of a new family of BTSC's and corresponding Cu(II) complexes, containing pendant cyclic tertiary amines of the piperidinyl or morpholinyl type, attached to the chelating framework using different alkyl linkers (Scheme 1). It has been described in the literature that weakly basic drugs positively charged are prone to localize in the acidic lysosome compartments and that these lysosomotropic properties can dictate a preferential cytotoxicity towards tumoral cells relative to normal cells, as many cancer cell types have a lysosomal acidification defect [40,41]. Additionally, the morpholine moiety has been used as a lysosome targeting group in fluorescent probes for imaging and tracking of lysosomes [42–44].

We expected that the presence of the cyclic amines could provide the complexes with lysomotropic properties, leading to an eventual enhancement of the uptake and retention in tumoral cells with a positive effect on the biological properties of Cu^{II}BSTC complexes as potential drugs for cancer theranostics. To tackle this goal, we have focused on this new family of Cu^{II}BTSC complexes that were synthesized using non-radioactive copper (^{nat}Cu) and ^{64}Cu, and were submitted to a thorough in vitro investigation that included: i) cyclic voltammetry experiments to assess influence of the pendant amines groups on the redox properties of the complexes; ii) DNA and human serum albumin (HSA) binding studies; iii) screening of the cytotoxicity for non-radioactive Cu^{II}BSTC complexes in a panel of human cancer cell lines; iv) cell uptake experiments for the corresponding radioactive ^{64}Cu^{II}BTSC complexes, using gamma-counting methods.

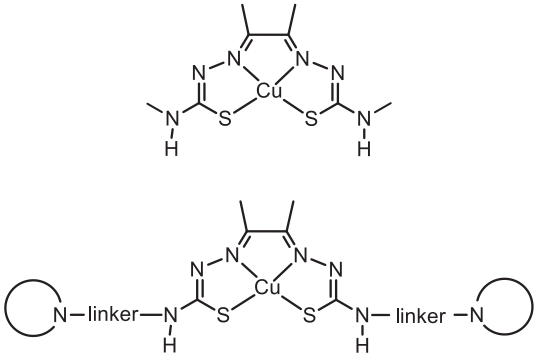

Scheme 1. Structure of Cu^{II}ATSM complex (top) and general structure of the new Cu^{II}BTSC complexes (bottom).

2. Results and discussion

2.1. Chemical and radiochemical synthesis

The work was initiated with the synthesis of the new chelators (**L^{1}**–**L^{4}**) (Scheme 2), which were obtained by an acid-catalyzed condensation reaction between 2.3-butanedione and the respective 4-substituted thiosemicarbazides (**1**–**4**), using methodologies similar to those described in the literature for related compounds [35]. It is important to notice that thiosemicarbazides **1**–**4** are relatively unstable and, for this reason, these compounds were used immediately after purification. The corresponding Cu^{II}BTSC complexes (**CuL^{1}** to **CuL^{4}**) were obtained in moderate to high yield (51–85%) by reacting copper acetate with one equivalent of the corresponding ligand in methanol, as depicted in Scheme 2. The Cu(II) complexes precipitate as reddish-brown microcrystalline solids.

The characterization of **CuL^{1}** to **CuL^{4}** was performed by ESI-MS, elemental analysis (CHN) and IR spectroscopy (details in the experimental part). Single crystals could be obtained for several of these compounds (**CuL^{1}**, **CuL^{3}** and **CuL^{4}**), which allowed the determination of their solid state structures by X-ray crystallography analysis. Crystals of **CuL^{1}**, **CuL^{3}** and **CuL^{4}** were obtained by slow diffusion of diethyl ether into a concentrated methanolic solution of the complexes. Single crystal X-ray diffraction analysis revealed that all the analyzed complexes exist in the solid state as discrete neutral molecules (Fig. 1). A summary of the crystallographic data is presented in Table S1. The most relevant bond distances and angles for all the complexes are listed in Table 1.

The bis(thiosemicarbazone) ligands are coordinated in a tetradentate fashion in all the complexes, through two of the imine nitrogen atoms and the two thiolate sulfur atoms, which results in the formation of three five-membered chelate rings (Fig. 1). As previously reported for related complexes, [45,46] the coordination geometry around Cu(II) in **CuL^{1}**, **CuL^{3}** and **CuL^{4}** is square planar, with a negligible distortion as indicated by the *cis* (80.25–85.74 Å) and *trans* (164.73–166.19 Å) angles around the metal. The standard deviation of the Cu atom from the least-square plane defined by the four donor atoms (S1 S2 N1 N4) is −0.0241, −0.0393 and 0.0217 Å for **CuL^{1}**, **CuL^{3}** and **CuL^{4}** respectively. Moreover, the central core of the molecules, constituted by the Cu atom and the two sulfur, six nitrogen and four carbon atoms of the ligand (Cu1 S1 S2 N1 N2 N3 N4 N5 N6 C1 C2 C3 C4) is also essentially planar (rms deviations of fitted atoms are 0.0222, 0.0595 and 0.0193 Å for compounds **CuL^{1}**, **CuL^{3}** and **CuL^{4}** respectively).

The Cu—S and Cu—N bond distances in the different complexes are comparable to the values reported for other Cu^{II}BTSC complexes [26,46–50]. The intraligand bond distances are also normal; in particular the C2—C3 bond lengths from the ethylenic bridge (1.464 to 1.509 Å) are also consistent with the values reported for other bis(thiosemicarbazonato) Cu(II) complexes with double backbone alkylation. The C—S bond lengths (1.735–1.7627 Å) are within the characteristic range for thiolate bonds [46–48].

As mentioned in the Introduction section, the ^{64}Cu counterparts of **CuL^{1}**-**CuL^{4}** were also synthesized for a more straightforward determination of the cellular uptake of the new Cu^{II}BTSC compounds in human tumoral cells. As shown in Scheme 3, the radiochemical syntheses of **^{64}CuL^{1}**-**^{64}CuL^{4}** was done by reacting $^{64}CuCl_2$ with the corresponding ligands at room temperature, as previously described for **^{64}Cu-ATSM** [35]. All the new ^{64}Cu-BTSC complexes were obtained in almost quantitative yield (>99%).

The chemical identity of the new radioactive Cu^{II}BTSC complexes was ascertained by comparing their analytical RP-HPLC gamma-traces

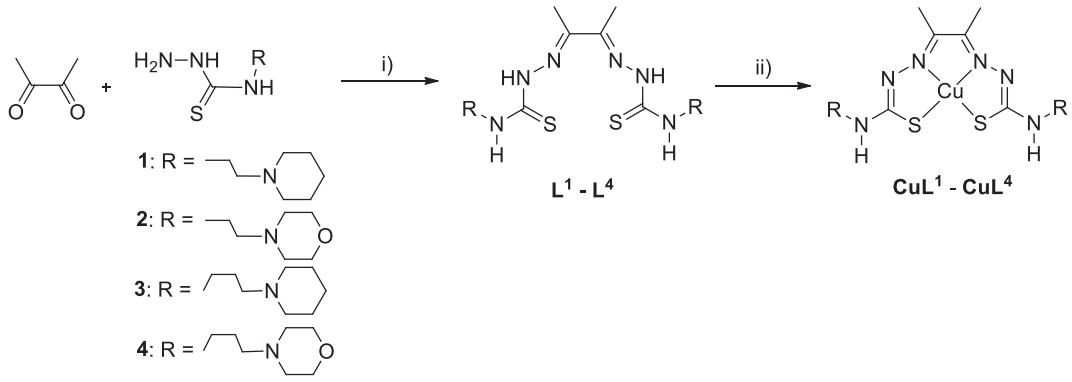

Scheme 2. Synthesis of the new BTSC chelators and respective Cu^{II} complexes (**CuL^1-CuL^4**). i) 5% acetic acid, 60 °C; ii) $Cu(OAc)_2.2H_2O$, MeOH, RT.

with the RP-HPLC UV–Vis traces of the analogues prepared with natural copper (**CuL^1-CuL^4**), as exemplified for **$^{64}CuL^4$** in Fig. 2.

The radioactive ^{64}Cu complexes were also used to assess the (lipo)hydrophilic character of the compounds. For that purpose, the partition coefficient of the complexes between n-octanol and 0.1 M PBS (pH 7.4) was determined by measurement of the ^{64}Cu radioactivity in the organic and aqueous phases. The respective log $D_{7.4}$ values are presented in the Experimental section (see Table 5). All the new Cu-^{II}BTSC complexes, with the exception of **CuL^4**, are less lipophilic than the parental **CuATSM** (log $D_{7.4} = 0.66$), at pH 7.4. Moreover, the piperidine-containing complexes (**CuL^1** (log $D_{7.4} = -0.23$) and **CuL^3** (log $D_{7.4} = -1.21$) are significantly more hydrophilic than the morpholine-containing counterparts (**CuL^2** (log $D_{7.4} = 0.02$) and **CuL^4** (log $D_{7.4} = 1.43$)). This difference certainly reflects the higher basicity of the piperidine ring compared to the morpholine one [51], as a consequence of the inductive effect (-I) due to the presence of the O atom in the later. As a result, the Cu(II) complexes must present different protonation degrees at pH = 7.4, being more predominant the non-protonated form for the morpholine derivatives, which might justify the increase of lipophilicity.

2.2. Electrochemistry

According to the literature, the electrochemical properties of Cu-^{II}BTSC complexes are largely dependent on small modifications of the di-imine backbone and, to a lesser extent, on the nature of the

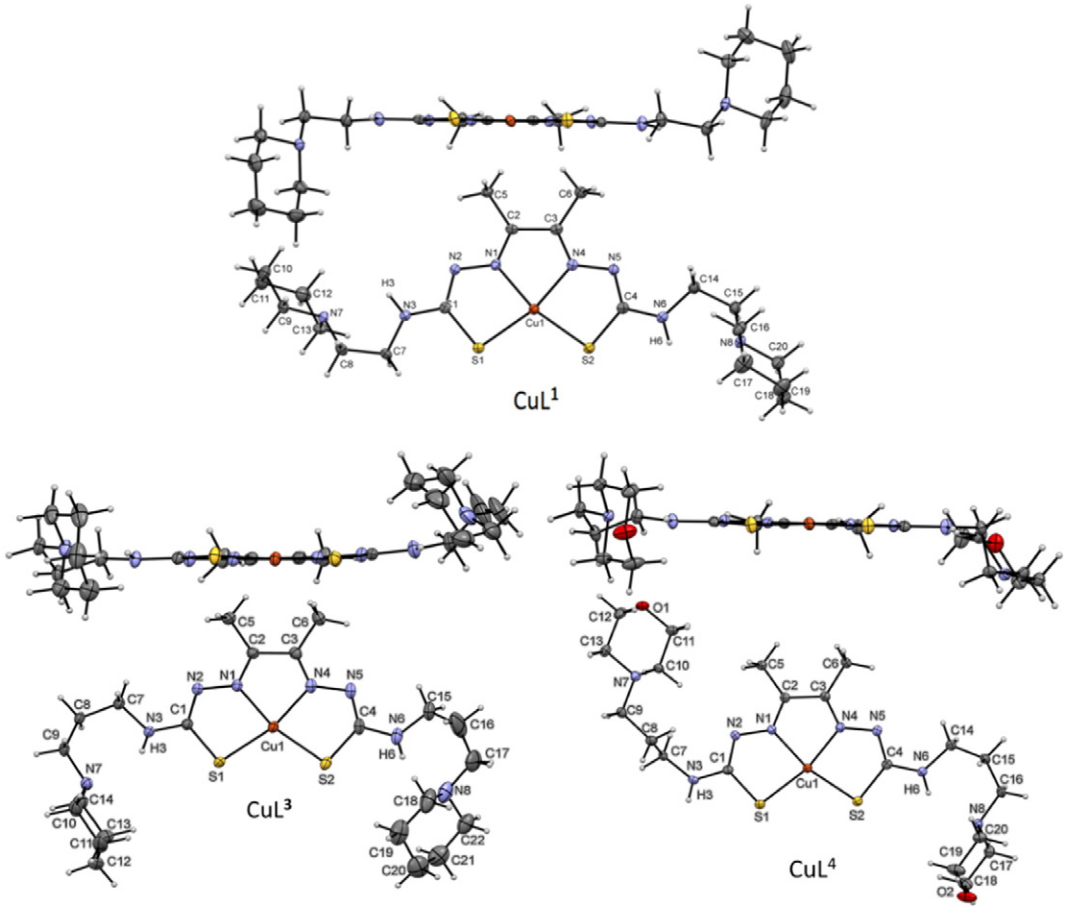

Fig. 1. ORTEP views (side and top views) of **CuL^1**, **CuL^3** and **CuL^4** with thermal displacement ellipsoids at the 50% probability level.

Table 1
Selected bond lengths (Å) and bond angles (°) for **CuL^1**, **CuL^3** and **CuL^4**.

Complex	**CuL^1**	**CuL^3**	**CuL^4**
Distances (Å)			
Cu—N1	1.955(2)	1.951(2)	1.9507(15)
Cu—N4	1.956(3)	1.973(3)	1.9615(15)1
Cu—S1	2.245(9)	2.2309(8)	2.2234(5)
Xu—S2	2.234(9)	2.2502(9)	2.2383(5)
N1—N2	1.358(3)	1.362(3)	1.368(2)
N4—N5	1.372(3)	1.366(4)	1.369(2)
N2—C1	1.318(4)	1.325(4)	1.328(2)
N5—C4	1.320(4)	1.327(4)	1.322(2)
C1—N3	1.343(4)	1.334(4)	1.331(3)
C4—N6	1.344(4)	1.340(4)	1.335(2)
C1—S1	1.748(3)	1.761(3)	1.7597(19)
C4—S2	1.752(3)	1.756(3)	1.7627(19)
C2—C3	1.473(4)	1.464(4)	1.483(3)
C2—C5	1.488(4)	1.494(4)	1.491(2)
C3—C6	1.477(4)	1.493(5)	1.489(2)
Angles (°)			
N1—Cu—S1	85.39(8)	85.02(8)	85.53(4)
N1—Cu—N4	80.37(10)	80.25(11)	80.54(6)
N4—Cu—S2	85.25(7)	85.24(8)	85.74(5)
S1—Cu—S2	108.95(3)	109.47(3)	108.173(19)
N1—Cu—S2	165.57(8)	165.48(8)	166.19(5)
N4—Cu—S1	165.72(7)	164.73(8)	166.05(5)
C1—S1—Cu	93.57(11)	94.06(11)	94.51(6)
C4—S2—Cu	94.11(10)	94.24(11)	93.78(6)

substituents attached at the terminal nitrogen atoms from the thiosemicarbazone functions [52]. Most importantly, the redox ability of this class of complexes is an important parameter that modulates their cellular retention and hypoxia selectivity.

In this sense, towards a better understanding of the biological behavior of the new complexes, the redox potentials of the couples $[Cu^{II}L]^0/[Cu^{I}L]^-$ were studied by cyclic voltammetry in dry DMSO at 20 °C, using $Ag/AgNO_3$ as the reference electrode and using the ferrocenium/ferrocene (Fe^+/Fe) couple as an internal reference. For comparative purposes, the redox potential of **CuATSM** was also measured in the same conditions. The electrochemical potentials of the complexes are shown in Table 2.

CuL^1-CuL^4 undergo a quasi-reversible process at negative potentials, spanning in the range −0.52 to −0.68 V vs. NHE (see Table 2 and Fig. 3). As invoked previously for the parental **CuATSM** [52], this process most likely involves a one-electron transfer that can be ascribed to the couple $[Cu^{II}L]^0/[Cu^{I}L]^-$. The $E_{1/2}$ values measured for **CuL^1-CuL^4** point

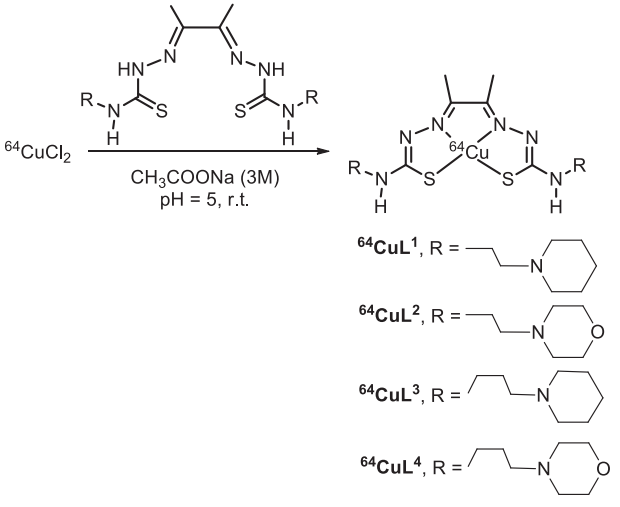

Scheme 3. Synthesis of the radioactive complexes **^{64}CuL^1-^{64}CuL^4**.

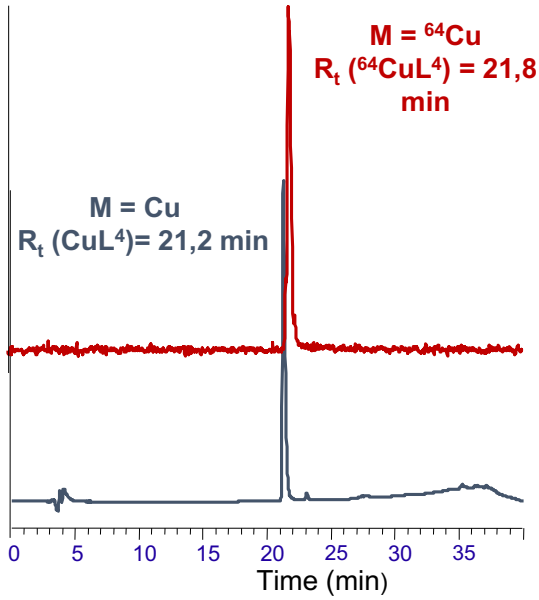

Fig. 2. HPLC chromatograms of **CuL^4** (UV detection, bottom HPLC trace) and **^{64}CuL^4** (γ detection, top HPLC trace).

out that the new Cu(II) complexes are likely to be hypoxia selective, such as the parental **CuATSM**.

For this reduction process, each complex exhibited a different separation (ΔEp = Ec-Ea/2) between the cathodic (Ec) and anodic (Ea) peaks. At a scan rate of 100 mV/s, the measured potential differences were 90, 227, 64, 193 and 135 mV for **CuATSM**, **CuL^1**, **CuL^2**, **CuL^3** and **CuL^4**, respectively. Despite the rather large peak separations observed for **CuL^1** and **CuL^3**, there is a decrease in peak intensity and a narrowing between the Ec and Ea values on their reduction waves, when the respective cyclic voltamograms are obtained with decreasing scan rates, from 500 to 20 mV/s. These results suggest that **CuL^1** and **CuL^3** follow the same quasi-reversible regime as complexes **CuATSM**, **CuL^2** and **CuL^4**.

The $E_{1/2}$ values of **CuL^2-CuL^4** span in a narrow range (−0.52 to −0.56 V vs. NHE) (see Table 2 and Fig. 3) and are almost coincident with the value of −0.54 V exhibited in our hands by **CuATSM**. For these complexes, the replacement of the methyl group at the N-terminus of the BTSC chelator by alkyl-piperidine or alkyl-morpholine derivatives, does not affect much the redox potentials. This trend agrees with results previously described by other authors for similar Cu^{II}BTSC complexes, also showing almost coincident $E_{1/2}$ values independently of the presence of alkyl substituents of different chain length at the N-terminal of the BTSC framework [52,53].

Table 2
$E_{1/2}$ for the $[Cu^{II}L]^0/[Cu^{I}L]^-$ redox process for the Cu^{II}BTSC complexes.

	$E_{1/2}$[a] ($[Cu^{II}L]^0/[Cu^{I}L]^-$) (V)		
Complex	vs. $Ag/AgNO_3$[b]	vs. NHE[c]	Relative to Fc^+/Fc couple[d]
CuATSM	−1.04	−0.54	−1.14
CuL^1	−1.18	−0.68	−1.26
CuL^2	−1.05	−0.55	−1.13
CuL^3	−1.05	−0.56	−1.14
CuL^4	−1.02	−0.52	−1.10

[a] Half-wave potentials are given by $E_{1/2} = (E_{pa} + E_{pc}) / 2$.
[b] The studies were performed under the same experimental conditions using working and counter Pt electrodes, $Ag/AgNO_3$ (10^{-3} M) as the reference electrode and DMSO as solvent. The scan rate used was 100 mV/s.
[c] $E_{1/2}$(vs. NHE) = $E_{1/2}$(vs. $Ag/AgNO_3$) + 498 mV [53].
[d] The redox potentials were normalized relatively to the Fc/Fc^+ couple, which was used as internal reference [54].

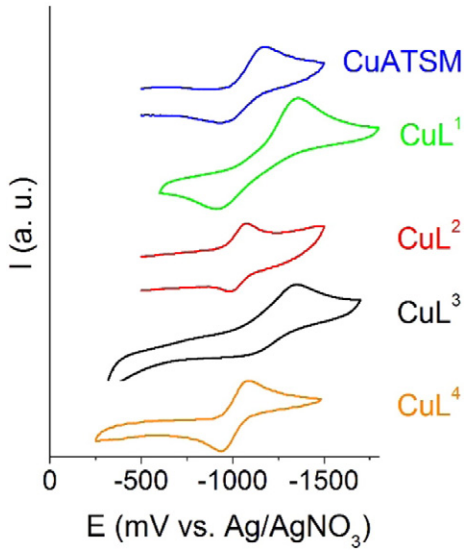

Fig. 3. Cyclic voltammograms of **CuATSM** and **CuL^1-CuL^4**. Scan rate 100 mV/s. Potentials are quoted relative to $Ag/AgNO_3$.

By contrast, **CuL^1** presented a more negative reduction potential (−0.68 V) showing that this complex is a weaker oxidant. Most probably, the reasons for this difference are associated with the possible formation of a more favorable intramolecular interaction, in solution, between Cu(II) and the nitrogen atom from the piperidinyl ring. This interaction increases the electronic density on the metal and, consequently, may contribute to decrease the reduction potential. The different behavior of **CuL^1** certainly reflects the better coordination capability of the piperidinyl nitrogen atom compared to the morpholine nitrogen atom, due to the electron withdrawing properties of the O-atom present in the morpholine [54]. In agreement with this reasoning, the two piperidinyl-containing complexes (**CuL^1**, $E_{1/2} = -0.68$ V; **CuL^3**, $E_{1/2} = -0,56$ V) are harder to reduce than the morpholinyl-containing counterparts (**CuL^2**, $E_{1/2} = -0.55$ V; **CuL^4**, $E_{1/2} = -0,52$ V).

Moreover, the length of the alkyl linker used to attach the N-heterocyclic rings to the BTSC's framework also affects the $E_{1/2}$ values. For each type of ring, the complexes displaying an ethyl linker show more negative $E_{1/2}$ values than the congeners having n-propyl linkers (**CuL^1** vs **CuL^3** and **CuL^2** vs **CuL^4**), which is most likely due to the influence of the size of the resulting chelating rings on the formation of intramolecular interactions involving the N-heterocyclic nitrogen atoms. In brief, the combination of the piperidine ring with the ethyl linker seems to favor the establishment of such intramolecular interaction, accounting for the redox behavior observed for **CuL^1**.

2.3. Interaction studies with biomolecules (HSA/DNA)

We have thought that the presence of peripheral protonable cyclic amines in complexes **CuL^1-CuL^4** could promote hydrogen bonding or electrostatic surface interactions with the negative phosphate groups on DNA or with the carboxylate and carbonyl functions of proteins, leading to an enhancement of the binding affinity towards these biological polymers. To address this issue, we have evaluated the interaction of **CuL^2** and **CuL^3**, containing morpholine and piperidine rings respectively, with HSA and calf-thymus DNA (CT-DNA) by fluorescence studies. For comparative purposes, the complex **Cu ATSM** was also tested using the same assays and under the same conditions.

The interaction of the Cu^{II}BTSC complexes with HSA was studied by direct fluorescence titration studies taking advantage from the fluorescence emission of HSA (maximum $\lambda_{em} = 351$ nm) when excited at 295 nm, due to the presence of a tryptophan residue at position 214 [55]. It is well described that the binding of molecules to HSA induces changes in the HSA emission intensity, as a consequence of alterations in the residues environment. The titrations of HSA with the Cu(II) complexes were carried out by adding increasing amounts of a 0.6 mM solution of each test compound to a TRIS buffered solution (pH 7.4) containing 1.5 μM HAS, after confirming that none of the complexes showed fluorescence emission when excited at 295 nm. We observed that the addition of the Cu^{II} complexes to the HSA solution resulted in moderate to strong emission quenching (as can be verified in the obtained titration curves (Fig. S1) and variation of the $\%I_F$ (at the maximum λ_{em}) (Fig. S2)).

The fluorescence quenching data of the BSA titrations were analyzed with the Stern–Volmer equation:

$$I_0/I = 1 + K_{SV}[Q] = 1 + k_q\tau_0[Q] \quad (1)$$

where I_0 and I are the fluorescence emission intensities in the absence and presence of quencher, respectively, and K_{sv}, [Q], k_q and τ_0 stand for the Stern–Volmer quenching constant, the quencher concentration (i.e. the Cu(II) complex conc.), the bimolecular quenching constant and the average lifetime of the biomolecule without quencher, respectively. Linear Stern-Volmer plots were obtained for all studied systems (see Fig. S3), which allowed the determination of the respective Stern-Volmer constants (Table 3).

To evaluate if the quenching of HSA fluorescence is due to binding of the compounds to HSA (static) or to collisional quenching (dynamic), the quenching constant, K_q, can be calculated, considering $\tau_0 = 10^{-8}$ s for HSA [56]. The K_q values are between $10^{12}-10^{13}$ M^{-1} s^{-1}, several orders of magnitude higher than the maximum diffusion-limited rate in water, [57] indicating that probably exists a static quenching due to the binding of the compounds to HSA.

The HSA titration data were also used to calculate the binding constant (K_a) and the number of binding sites (n) per HSA molecule, considering that the Cu(II) complexes under study bind independently to a set of equivalent sites. Under this hypothesis, the equilibrium between free and bound molecules is given by Eq. (2). Fig. S4 shows the plots obtained by adjustment of our data to Eq. (2), and the values calculated for K_a and n are listed in Table 3.

$$\log[(I_0-I)/I] = \log K_a + n\log[Q] \quad (2)$$

The binding interaction of the copper complexes with calf-thymus DNA (CT-DNA) was also evaluated. For that purpose, fluorescence competition titrations were done with a fluorescent dye, thiazole orange (TO), a known DNA intercalator [58]. The studies were initiated with the optimization of the TO:DNA ratio to maximize the fluorescence emission. It was found that the saturation of the emission spectra occurred at ca. 0.7:1 molar ratio; thus, this was the ratio used in all assays. The fluorescence emission spectra were measured in all systems for a TO:DNA = 0.7:1 ratio and with increasing amounts of each complex (Fig. S5). In all cases, there is a quenching on fluorescence, indicating that the complexes are able to compete with TO for the same binding sites, or interact with DNA at different sites. The use of the Stern-Volmer formalism (see Eq. (1)) allowed the determination of the K_{SV} constants based on the DNA titrations. The plots of these data are not linear in the entire measured concentration range, and the curves reach a plateau for ratios [Cu]:[TO] ≅ 2 (Fig. S6). Therefore, only the initial linear regions

Table 3
Stern–Volmer constants (Ksv) and R^2 (from SV plot) for the interaction of the Cu(II) complexes with HSA[a] and CT-DNA[b]; binding constants (K_a), number of binding sites on HSA (n) and R^2 (from K_a fitting) for their interaction with HSA.

Compound	$10^{-4}K_{SV}(M^{-1})$	R^2	$10^{-3}K_a(M^{-1})$	n	R^2
CuATSM	6.1[a]/1.5[b]	0.969[a]/0.978[b]	9.3	0.87	0.988
CuL^2	1.1[a]/1.6[b]	0.971[a]/0.910[b]	2.1	0.86	0.966
CuL^3	3.7[a]/1.1[b]	0.964[a]/0.981[b]	7.9	0.75	0.937

were used to determine the K_{SV} constants for **CuATSM**, **CuL^2** and **CuL^3**. The calculated constants are presented in Table 3.

In summary, the K_{sv} values for the different complexes are all of the same order of magnitude, either for the HSA or CT-DNA binding, and span between 1.1×10^{-4} and 6.1×10^{-4} M^{-1} (Table 3) pointing out for compounds with moderate affinity towards these biomolecules. For the HSA interaction, the binding constant of **CuATSM** ($K_a = 9.3 \times 10^{-3}$ M^{-1}) is larger than those observed for **CuL^2** and **CuL^3** ($K_a = 2.1 \times 10^{-3}$ and 7.9×10^{-3} M^{-1}, respectively) showing that the presence of the protonable cyclic amine groups did not increase the binding activity by promoting electrostatic interactions. Apparently, the introduction of bulkier groups in the ligands structure decreases the ability of the complexes to bind the protein, probably due to steric hindrance. This is in agreement with results previously reported for other bis(thiosemicarbazonato) Cu(II) complexes, for which the introduction of bulky aliphatic substituents at the N-terminus of the chelator framework reduces their HSA binding affinity [59,60].

2.4. Biological evaluation

To have an insight on the antitumoral properties of the new Cu^{II}BTSC complexes, their cytotoxic activity in human cancer cells lines was assessed and compared with that of **CuATSM** and respective chelators. A diverse panel of human cancer cell lines was used: ovarian carcinoma - sensitive (A2780) and resistant (A2780cisR) to cisplatin; cervical adenocarcinoma (HeLa) and breast adenocarcinoma (MCF-7). Moreover, the cytotoxic activity was also studied in human non-tumoral cells (HEK 293). Searching to rationalize the trends on the cytotoxic activity of the compounds, these cell studies comprised also the evaluation of their quantitative cell uptake based on gamma-counting measurements with the ^{64}Cu-BTSC complexes.

2.4.1. Cytotoxicity in human cancer cell lines

In the cytotoxicity studies, cells were incubated with increasing concentrations of the different ligands and complexes for 48 h at 37 °C, and the cellular viability was evaluated by the MTT assay. The inhibition of growth (%) was calculated and the IC_{50} values (i.e., concentration which reduces the growth by 50%) were determined. The results are presented in Table 4.

The new Cu^{II}BTSC complexes (**CuL^1**-**CuL^4**) exhibit sub-micromolar IC_{50} values against all cancer cell lines, ranging between 0.21 and 0.82 μM. These values indicate a rather pronounced cytotoxicity for all the tested compounds, and can be considered comparable to those reported by other authors for the activity of **CuATSM** in other human tumoral cell lines [52]. There is a clear effect of metal-complexation on the cytotoxic profile of the compounds, as the Cu(II) complexes are much more cytotoxic than the corresponding ligands.

Most importantly, **CuL^1**-**CuL^4** display a similar activity in cisplatin-sensitive A2780 and cisplatin-resistant A2780cisR cell lines, indicating that the new Cu(II) complexes were in general able to circumvent cisplatin cross-resistance, in contrast with **CuATSM** that is roughly two times more active in the sensitive cell line. All the compounds present similar antiproliferative properties against the human non-tumoral HEK 293 cell line and the tested tumoral cell lines, pointing out for relatively low therapeutic indices.

2.4.2. Cellular uptake and retention

In order to evaluate the influence of the cyclic amine groups on the cell permeability/entrance of the Cu^{II}-BTSC complexes, cellular uptake studies were performed using the radioactive complexes **^{64}CuATSM** and **^{64}CuL^1**-**^{64}CuL^4**, profiting from the straightforward quantification of the radioactivity associated with the cells through gamma-counting measurements. These studies were performed with A2780 and MCF-7 cells, which were incubated with the ^{64}Cu complexes at 37 °C at different time points over a 4 h period. After incubation and cell lysis, the activity associated to the lysate was measured and the cellular uptake of the different complexes calculated as the percentage of uptake per total applied activity, as a function of incubation time (Fig. 4).

In both cell lines, the complexes showed a similar behavior with the cellular uptake increasing as a function of incubation time at 37 °C. **^{64}CuATSM** presented a significantly lower value of uptake after 4 h incubation (10.4 ± 0.2% and 10.5 ± 1.3% in A2780 and MCF-7 cells, respectively), when compared with **CuL^1**-**CuL^4** that showed a faster entrance into the cells. Among them, **^{64}CuL^1**, containing the piperidine group attached to the chelator by the shorter ethylenic linker, showed the best ability to enter into the tumoral cells studied, reaching values of cellular uptake of 24.7 ± 0.1% and 32.9 ± 1.3% in A2780 and MCF-7 cells, respectively, at 4 h of incubation.

^{64}CuL^1-**^{64}CuL^4** showed an augmented cell uptake when compared with the smallest and lipophilic **^{64}CuATSM**. Remarkably, all the new complexes are more hydrophilic than **^{64}CuATSM**, with the exception of **^{64}CuL^4**. Previous attempts have been described to obtain water-soluble and more hydrophilic **CuATSM** derivatives, aiming at the design of metallodrugs/radiopharmaceuticals with more favorable physicochemical properties [61,62]. However, to the best of our knowledge, all of them have presented a lower cellular uptake than **CuATSM**. Taken together, these results suggest that the presence of the cyclic amines with protonable nitrogen atoms induce an enhancement of cellular uptake.

We have reasoned that the enhanced cell uptake observed for **^{64}CuL^1**-**^{64}CuL^4** could result from the association of the complexes to the cell membrane without occurrence of extensive internalization of the complexes. To clarify this aspect, we have performed cell internalization studies for the complex that presented the highest cell uptake, **^{64}CuL^1**, using the MCF-7 cell line. In this type of experiment, we are able to distinguish between membrane-associated and internalized (i.e. intracellular) activities. As can be seen in Fig. 5, there is a considerable amount of radioactivity associated with the membrane for the

Table 4
IC_{50} (μM) values of the Cu^{II}BTSC complexes and respective ligands, as determined by the MTT assay after 48 h of incubation of the compounds at 37 °C with tumoral (A2780, A2780cisR, HeLa, MCF-7) and non-tumoral cells (HEK293).

Compound	IC_{50} (μM)				
	Non-tumoral cells	Tumoral cells			
	HEK293	A2780	A2780cisR	HeLa	MCF-7
ATSM	105.9 ± 25.6	155.4 ± 36.9	>200	–	–
L^1	108.4 ± 44.7	>200	>200	–	–
L^2	161.0 ± 61.0	>200	>200	–	–
L^3	>200	>200	>200	–	–
L^4	>200	>200	>200	–	–
CuATSM	1.26 ± 0.38	0.37 ± 0.07	0.87 ± 0.11	0.76 ± 0.27	0.74 ± 0.25
CuL^1	0.84 ± 0.78	0.58 ± 0.19	0.30 ± 0.09	0.40 ± 0.10	0.27 ± 0.07
CuL^2	0.86 ± 0.18	0.42 ± 0.08	0.54 ± 0.05	0.82 ± 0.32	0.72 ± 0.19
CuL^3	0.51 ± 0.17	0.28 ± 0.06	0.39 ± 0.06	0.34 ± 0.10	0.73 ± 0.24
CuL^4	0.24 ± 0.04	0.21 ± 0.04	0.26 ± 0.04	0.29 ± 0.10	0.39 ± 0.15

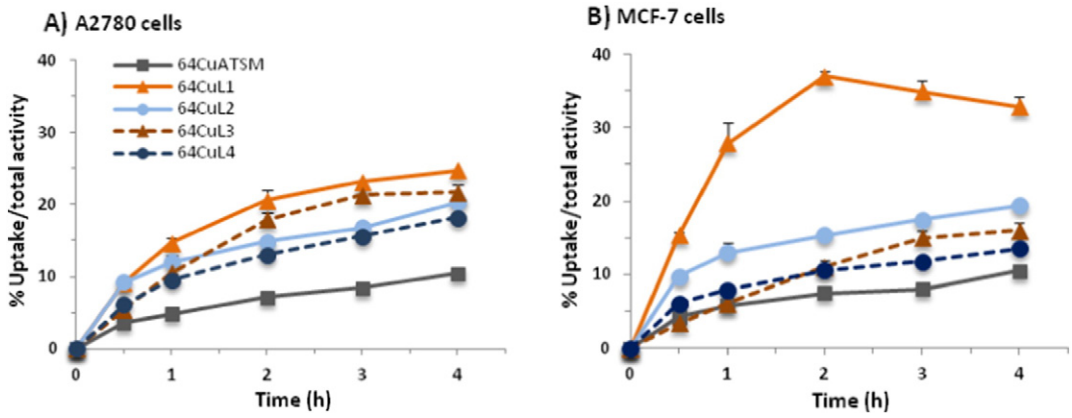

Fig. 4. Cellular uptake of ^{64}Cu-complexes in A) A2780 and B) MCF-7 cells. ^{64}Cu-Complexes containing a cyclic amine group: ▲ piperidine group (^{64}**CuL^{1}** and ^{64}**CuL^{3}**); ● morpholine group (^{64}**CuL^{2}** and ^{64}**CuL^{4}**).

shortest incubation times but, even for these early points, most of the cell-associated radioactive complex is already internalized by the cell. Thereafter, there is a fast release of ^{64}**CuL^{1}** from the membrane with increasing internalization, until reaching a plateau. The internalization rate seems faster for ^{64}**CuL^{1}** than ^{64}**CuATSM** (Fig. 5). For the later, the amount associated with the membrane is constant along the time and there is a slower increase of the internalized complex. These results confirmed that the presence of the protonable cyclic amine groups promotes an increase of the rate of the internalization process.

Furthermore, we have performed efflux experiments in A2780 and A375 cells for ^{64}**CuL^{1}** and ^{64}**CuL^{2}**, in comparison with the parental complex ^{64}**CuATSM**, in order to understand how the presence of the pendant cyclic amines affects the intracellular retention of the Cu^{II}BTSC complexes. Cells were incubated with ^{64}Cu-complexes for 3 h at 37 °C to allow the cellular uptake to occur, and then washed and re-incubated with culture medium to determine the efflux of ^{64}**CuL^{1}**. The cellular retention of the complexes, expressed in percentage of total initial uptake, is presented in Fig. 6.

A moderate washout was observed for all complexes in both cell lines, with cells incubated with ^{64}**CuL^{1}** and ^{64}**CuL^{2}** showing about 40% of internalized activity, after 5 h. Nevertheless, the efflux rate seems faster in the A2780 cell line for early time points. Noticeably the cellular retention pattern of ^{64}**CuL^{1}** and ^{64}**CuL^{2}** was almost coincident with that exhibited by ^{64}**CuATSM**. This result indicates that, if the pendant cyclic amine appeared to have a role in the kinetics (or mechanism) of entrance into the cells, it does not seem to modulate the cellular efflux mechanism.

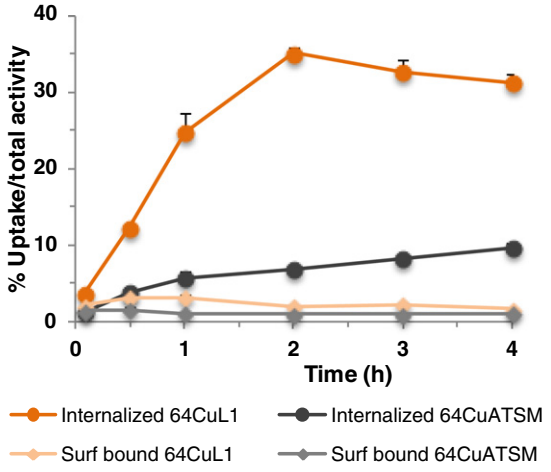

Fig. 5. Internalization and surface binding of ^{64}Cu-complexes (^{64}**CuL^{1}** and ^{64}**CuATSM**) in MCF-7 breast cancer cells.

It has been reported a correlation between the ^{64}Cu release and Cu$^{II/I}$ redox potentials in agreement with a redox potential-dependent intracellular reductive trapping [52]. The Cu$^{II/I}$ redox potential of the Cu complexes reported in this work did not differ significantly from the parental **CuATSM** (see Electrochemistry results). Apparently, this similitude could justify that no difference was detected in their cell efflux. However, it is hardly conceivable that a much polar and hydrophilic complex like ^{64}**CuL^{1}** would show, in its intact form, back-diffusion rate almost coincident with that of ^{64}**CuATSM**.

Other authors have proposed that the efflux of ^{64}**CuATSM** from the cells can be a more complicated process that might not involve necessarily the back-diffusion of the intact complex from the cell, based on the clear influence of different cell lines in the efflux rate [32]. They have considered that the reduction of ^{64}**CuATSM**, even under normoxic conditions, leads to the formation of ^{64}Cu^{I} and release of the chelator. The Cu^{I} ion once absorbed into the intracellular Cu pool, undergoes the intrinsic cellular metabolism of copper. In particular, there are two primary copper exporters, the P-type ATPases ATP7A (Menkes protein) [63] and ATP7B (Wilson protein) [64], which are specific for Cu(I) and might mediate the efflux of ^{64}Cu^{I} from the cells by active transport. Our results seem to indicate that this type of active transport is most likely involved in the efflux of Cu^{II}BTSC complexes from the cells, as ^{64}**CuL^{1}**, ^{64}**CuL^{2}** and ^{64}**CuATSM** presented identical efflux rates despite having different physico-chemical properties (e.g. size, acid-base properties or lipophilicity). Thus, a mechanism other than the model of redox potential-dependent intracellular reductive trapping is probably involved in the higher accumulation of the ^{64}**Cu^{II}BTSC** complexes containing pendant cyclic amines.

In brief, we can speculate that the inclusion of protonable tertiary amine could provide the new compounds with a higher affinity towards the cell membrane, promoting the endocytosis process with enhanced cell uptake and possibly leading to the lysosomal trafficking of the compounds [65]. In this scenario, these new ^{64}**Cu^{II}BTSC** complexes would benefit from an increased cellular accumulation, albeit with efflux rates similar to ^{64}**CuATSM**. Alternatively, the non-protonated form of the complexes could be the responsible for enhancement of cell uptake. These free forms are in equilibrium with the protonated ones, and present an intrinsically higher lipophilicity than **CuATSM** that could facilitate the diffusion through the cell membrane. At physiological pH, ^{64}**CuL^{4}** ($\log D_{7.4} = 1.43$) presents a higher lipophilicity than ^{64}**CuL^{1}** ($\log D_{7.4} = -0.23$), which is consistent with the predominance of the free form in solution in the case of **CuL^{4}**. However, ^{64}**CuL^{1}** showed a much higher cell uptake than ^{64}**CuL^{4}**, particularly in the MCF-7 cell line, which does not corroborate an important role of the lipophilicity of the non-protonated form of the complexes on their entrance into the cells.

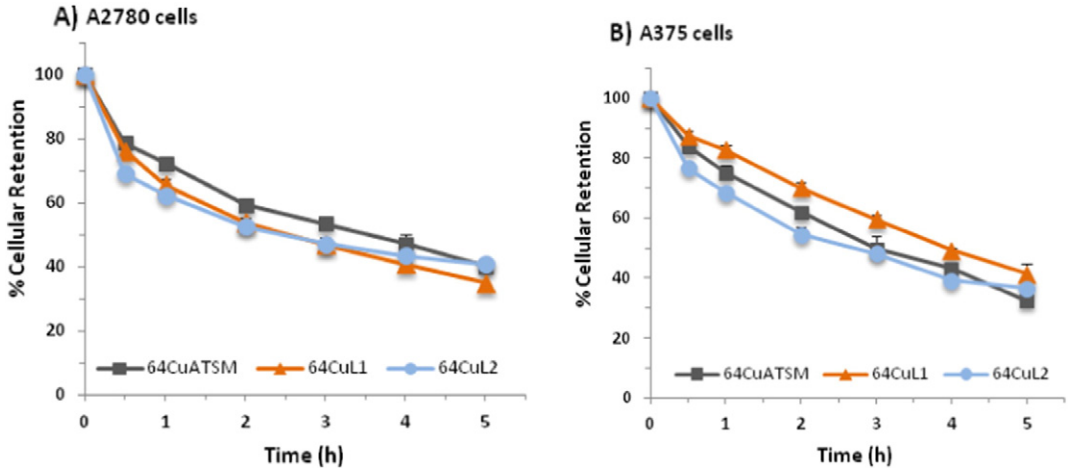

Fig. 6. Cellular efflux of ^{64}Cu-complexes in A2780 ovarian carcinoma (A) and A375 melanoma (B) cells. ^{64}Cu-complexes containing a cyclic amine group: ▲ piperidine group (**^{64}CuL^{1}**); ● morpholine group (**^{64}CuL^{2}**).

3. Conclusions

In this contribution a series of Cu(II) complexes (**CuL^{1}-CuL^{4}**) with novel bis(thiosemicarbazone) ligands, bearing pendant piperidine and morpholine groups, was synthesized and their anticancer activity evaluated in a panel of human tumor cell lines, together with the measurement of the corresponding cell uptake and rate of efflux.

The presence of the protonable cyclic amines did not led to an enhancement of the interaction of the complexes with HSA or CT-DNA, being more prevalent the bulkiness of the substituents rather than the presence of localized positive charges at the N-heterocyclic rings. However, **CuL^{1}-CuL^{4}** showed a remarkably augmented cellular uptake compared with **CuATSM**, probably due to a faster internalization of the complexes.

The augmented cell uptake of **CuL^{1}-CuL^{4}** was not reflected in an increased cytotoxic activity when compared with **CuATSM**, but unlike **CuATSM**, **CuL^{1}-CuL^{4}** surpassed cisplatin cross-resistance. We also anticipate that the favorable cell uptake values of the radioactive **^{64}CuL^{1}**-**^{64}CuL^{4}** will certainly potentiate strong radiotoxic effects, which is currently under investigation within our interest on the design of novel tools for radionuclide therapy of cancer.

Despite the continued development of Cu^{II}BTSC complexes as potential metallodrugs for cancer theranostics, many aspects of the mechanisms involved in cell uptake, intracellular trafficking, distribution and efflux of this family of compounds still need to be elucidated. Further work is warranted to understand how the pendant cyclic amines influence each of those mechanisms in the case of **CuL^{1}-CuL^{4}**. Particularly interesting will be to perform more detailed studies to understand if the increased cellular uptake observed is related to a lysosomal accumulation of these complexes.

4. Experimental section

4.1. Materials and methods

All chemicals were p.a. grade and were used without purifications unless stated otherwise. The complex **CuATSM** was synthesized as described in the literature [35,66]. The chemical reactions were followed by TLC. ^{1}H and ^{13}C NMR spectra were recorded on a Varian Unity 300 MHz or 400 MHz spectrometer at the frequencies of 300 or 400 MHz (^{1}H) and 75 or 100 MHz (^{13}C), respectively. ^{1}H and ^{13}C chemical shifts (δ) are reported in ppm relative to residual solvent signals ($CDCl_3$: 7.26 ppm for ^{1}H NMR, 77.0 ppm for ^{13}C NMR; DMSO-d_6: 2.50 ppm for 1H NMR, 39.52 for ^{13}C NMR; CD_3OD: 3.31 ppm for ^{1}H NMR, 49.00 ppm for ^{13}C NMR). Electrospray ionization mass spectrometry (ESI-MS) was performed on a QITMS instrument in positive and negative ionization mode. Elemental analyses were recorded on an EA 110 CE automated instrument. IR spectra were recorded in KBr pellets on a Bruker Tensor 27 spectrometer.

Thin-layer chromatography (TLC) was performed on plates of precoated silica plates 60 F_{254} (Merck). Visualization of the plates was carried out using UV light (254 nm) and/or iodine chamber. Gravity column chromatography was carried out on silica gel (Merck, 70–230 mesh).

Reversed-phase high performance liquid chromatography (RP-HPLC) analyses of natural and radioactive copper complexes were performed with a Perkin Elmer LC pump 200 coupled to a LC 290 tunable UV–vis detector and to a Berthold LB-507A radiometric detector. A Macherey-Nagel C18 reversed-phase column (Nucleosil 5 mm, 250 × 4 mm) was used. HPLC solvents consisted of 0.1% CF_3COOH in H_2O (solvent A) and 0.1% CF_3COOH solution in methanol (solvent B), gradient: t = 0–25 min, 10–90% eluent B; 25–27 min, 90–100% eluent B; 27–30 min, 100% eluent B; 30–32 min, 100–10% eluent B; 32–40 min, 10% eluent B.

4.2. General synthesis of 4-N-substituted 3-thiosemicarbazides (1–4) [67,68]

To an aqueous solution of NaOH (1.0 M, 3.3 mL), containing 1 mmol of the desired amine (2-(piperidin-1-yl)ethylamine, 3-(piperidin-1-yl)propylamine, 2-morpholinoethylamine or 3-morpholinopropylamine) was added carbon disulfide (1.4 mmol) at RT and the reaction mixture was stirred for several hours (19–43 h). Then, sodium chloroacetate (1 mmol) was added and the reaction mixture was kept under stirring for further 24–45 h at RT. The orange color of the reaction mixture turned yellow. Finally, an excess of hydrazine (9.5 mmol) was added and the reaction mixture was refluxed for 5 h, until completely colorless. After cooling down, the reaction mixture was extracted with ethyl acetate (4 × 25 mL). The organic phase was dried over Na_2SO_4, and filtered to afford the desired products: 4-(2-(piperidin-1-yl)ethyl)-3-thiosemicarbazide (**1**), 4-(2-(morpholin-1-yl)ethyl)-3-thiosemicarbazide (**2**), 4-(3-(piperidin-1-yl)propyl)-3-thiosemicarbazide (**3**), and 4-(3-(morpholin-1-yl)propyl)-3-thiosemicarbazide (**4**).

Under our experimental conditions, we have verified that the thiosemicarbazide derivatives **1**–**4** are relatively unstable; therefore, these compounds were used immediately in the synthesis of **L^{1}-L^{4}**, after the appropriate work-up to obtain **1**–**4**. For this reason, we did not proceed with the detailed chemical characterization of **1**–**4**.

4.3. General procedure for the synthesis of diacetyl-2-bis(4-N-substituted-3-thiosemicarbazone) (L^1–L^4)

The desired 4-*N*-substituted-3-thiosemicarbazide (2.5 mmol) was dissolved in 4.3 mL of distilled water containing 5% acetic acid at 60 °C. Then, 2.3-butanedione (0.5 mL, 1 mmol) was added dropwise and the reaction was stirred overnight at RT. Triethylamine was then added until basic pH (ca. 8–9). The aqueous phase was diluted with water (50 mL) and was extracted with dicloromethane (2 × 50 mL). The organic phase was dried over Na_2SO_4, filtered and the concentrate was submitted to column chromatography on silica gel (CH_2Cl_2/MeOH/Et_3N 1:0.05:0.01) to give a yellowish solid, which was further washed with dicloromethane and *n*-hexane.

Diacetyl-2-bis[4-*N*-(2′-(piperidin-1-yl)ethyl)-3-thiosemicarbazone (L¹) – Yield = 57%; R_f (DCM:MeOH:TFA 1:0.1:0.01) = 0.20; ^{1}H NMR (DMSO-d_6, 400 MHz) δ: 1.40 (m, 4H), 1.50 (m, 8H), 2.12 (m, 2H), 2.21 (s, 6H), 2.38 (m, 8H), 3.59 (m, 6H), 8.37 (t, 2H, *J* = 6.0 Hz), 10.43 (s, 2H); ^{13}C NMR (DMSO-d_6, 100 MHz) δ: 12.67 (CH_3), 25.02, 26.57, 41.51, 54.72, 57.19, 148.34 (C = N), 178.34 (NHC = S); **ES⁺ MS** $C_{20}H_{38}N_8S_2$ (454.27) *m/z* 455.5 $[M + H]^+$; Anal. calcd. for $C_{20}H_{38}N_8S_2$: C 52.83, H 8.42, N 24.65; found C 52.89, H 8.70, N 24.59; IR (KBr, ν/cm^{-1}): 3298 (m, N—H), 3167 (m, N—H), 2934 (m sharp), 1536 (vs, C═N), 1490 (vs, C═N), 1247 (s, thioamide), 1214 (s), 1152 (m, N—N), 1114 (mw), 711 (w). (vs, very strong; s, strong; m, medium; w, weak; sh, sharp).

Diacetyl-2-bis[4-*N*-(2′-(morpholinoethyl)-3-thiosemicarbazone (L²) – Yield = 32%; R_f (DCM:MeOH:TFA 1:0.1:0.01) = 0.21; ^{1}H NMR (DMSO-d_6, 300 MHz) δ: 2.25 (s, 6H, CH_3), 2.46 (m, 8H), 3.61 (m, 8H), 3.69 (m, 4H), 8.42 (t, 2H, *J* = 3.0 Hz, NH), 10.49 (s, 2H, NH), 4H under the residual peak of DMSO; ^{13}C NMR (DMSO-d_6, 75 MHz) δ: 12.47 (CH_3), 41.18, 53.71, 56.94, 67.05, 148.51 (C = N), 178.45 (NHC = S); ES$^+$ MS $C_{18}H_{34}N_8O_2S_2$ (458.22) *m/z* 459.4 $[M + H]^+$; Anal. calcd. for $C_{18}H_{34}N_8O_2S_2.0{,}5H_2O$: C 46.23, H 7.54, N 23.96; found C 46.30, H 7.62, N 23.92; IR (KBr, ν/cm^{-1}): 3335 (s, N—H), 3278 (w, N—H), 2862 (w), 2807 (m), 1532 (vs, C═N), 1489 (vs, C═N), 1234 (s, thioamide), 1203 (s), 1138 (N—N), 765 (m), 616 (m).

Diacetyl-2-bis[4-*N*-(3′-(piperidin-1-yl)propyl)-3-thiosemicarbazone (L³) – Yield = 55%; R_f (DCM:MeOH:TFA 1:0.1:0.01) = 0.24; ^{1}H NMR (DMSO-d_6, 300 MHz) δ 1.40 (m, 4H), 1.51 (m, 8H), 1.76 (m, 4H), 2.24 (s, 6H), 2.30 (m, 12H), 3.62 (m, 4H), 8.41 (t, 2H, *J* = 3.0 Hz), 10.23 (s, 2H); ^{13}C NMR (DMSO-d_6, 75 MHz) δ: 12.69 (CH_3), 25.11, 26.47, 26.86, 43.44, 55.03, 57.22, 148.84 (C = N), 178.54 (NHC = S); ES$^+$ MS $C_{22}H_{42}N_8S_2$ (482.2) *m/z* 483.7 $[M + H]^+$; Anal. calcd. for $C_{22}H_{42}N_8S_2.H_2O$: C 52.76, H 8.86, N 22.38; found C 52.76, H 8.90, N 22.46; IR (KBr, ν/cm^{-1}): 3340 (m, N—H), 3163 (m, N—H), 2941 (s), 1539 (vs, C═N), 1496 (vs, C═N), 1212 (s, thioamide), 1146 (s, N—N), 1085 (m), 606 (w), 555 (w).

Diacetyl-2-bis[4-*N*-(3′-(morpholinopropyl)-3-thiosemicarbazone (L⁴) – Yield = 52%; R_f (DCM:MeOH:TFA 1:0.1:0.01) = 0.10; ^{1}H NMR (DMSO-d_6, 400 MHz) δ: 1.78 (t, 4H), 2.24 (s, 6H), 2.38 (m, 12H), 3.46 (m, 12H), 8.42 (t, 2H, *J* = 3.0 Hz, NH), 10.22 (s, 2H, NH); ^{13}C NMR (DMSO-d_6, 100 MHz) δ: 11.82 (CH_3), 25.68, 42.24, 53.39, 56.09, 66.23, 148.01 (C = N), 177.75 (NHC = S); ES$^+$ MS $C_{20}H_{38}N_8O_2S_2$ (486.26) *m/z* 487.4 $[M + H]^+$; Anal. calcd. for $C_{20}H_{38}N_8O_2S_2.CH_3OH$: C 48.62, H 8.16, N 21.61; found C 48.51, H 8.27, N 21.67; IR (KBr, ν/cm^{-1}): 3338 (w, N—H), 3219 (M, N—H), 2954 (w), 2854 (w), 1535 (vs, C═N), 1488 (vs, C═N), 1203 (vs, thioamide), 1117 (vs, N—N), 557 (m, broad).

4.4. General procedure for the synthesis of aliphatic bis(thiosemicarbazonato) copper (II) complexes

To a suspension of the bis(thiosemicarbazone) ligand (**L¹**–**L⁴**; 0.2–0.4 mmol) in methanol (5 mL) was added one equivalent of copper acetate monohydrate (0.2–0.4 mmol) and the mixture was stirred under RT overnight. To obtain **CuL¹** and **CuL⁴** the solvent of the reaction mixture was concentrated to dryness under vacuum and the residue was dissolved in dimethylformamide (**CuL¹**) or dichloromethane (**CuL⁴**). The complexes precipitated as orange-brown solids upon addition of dyethylic ether. In case of **CuL²** and **CuL³**, the methanolic solution was concentrated and after addition of dyethylic ether, the complexes precipitated and were collected by filtration as dark-brown solids.

Copper Diacetyl-2-bis[4-*N*-(2′-(piperidin-1-yl)ethyl)-3-thiosemicarbazonato (CuL¹): Yield: 51%. ES$^+$ MS for $C_{20}H_{36}CuN_8S_2$ (515.18), *m/z*: 516.3 $[M + H]^+$; Anal. calcd. for $C_{20}H_{36}CuN_8S_2.1H_2O$: C 44.96, H 7.17, N 20.98; found C 44.93, H 7.30, N 20.91; IR (KBr, ν/cm^{-1}): 3405 (s sharp, N—H), 3340 (m sharp) 2929 (vs sharp), 1477 (vs, C═N), 1224 (s, thioamide), 1124 (w, N—N), 1047 (w), 841 (w, C—S), 756 (w).

Copper Diacetyl-2-bis[4-*N*-(3′-(morpholinopropyl)-3-thiosemicarbazonato (CuL²): Yield: 55%. ES$^+$ MS for $C_{18}H_{32}CuN_8O_2S_2$ (519.1), *m/z*: 520.3 $[M + H]^+$; Anal. calcd. for $C_{18}H_{32}CuN_8O_2S_2$: C 41.56, H 6.20, N 21.55; found: C 41.53, H 6.22, N 21.60; IR (KBr, ν/cm^{-1}): 3324 (vs broad, N—H), 2953 (s), 2812 (s), 1510 (vs, C═N), 1231 (vs, thioamide), 1114 (vs, N—N), 865 (m, C—S), 611 (w).

Copper Diacetyl-2-bis[4-*N*-(3′-(piperidin-1-yl)propyl)-3-thiosemicarbazonato (CuL³): Yield: 78%. ES$^+$ MS for $C_{22}H_{40}CuN_8S_2$ (543.2), *m/z*: 544.4 $[M + H]^+$; Anal. calcd. for $C_{22}H_{40}CuN_8S_2.H_2O$: C 46.99, H 7.53, N 19.93, found: C 47.02, H 7.43, N 19.96; IR (KBr, ν/cm^{-1}): 3220 (s broad, N—H), 2934 (s sharp), 1500 (vs, C═N), 1430 (s), 1221 (s, thioamide), 1123 (m, N—N), 757 (m, C—S), 627 (w).

Copper Diacetyl-2-bis[4-*N*-(2′-(morpholin-1-yl)ethyl)-3-thiosemicarbazonato (CuL⁴): Yield: 85%. ES$^+$ MS for $C_{20}H_{36}CuN_8O_2S_2$ (547.2), *m/z*: 548.4 $[M + H]^+$; Anal. calcd. for $C_{20}H_{36}CuN_8O_2S_2$: C 43.81, H 6.62, N 20.44, found: C 43.87, H 6.73, N 20.49; IR (KBr, ν/cm^{-1}): 3349 (vs, N—H), 2943 (s), 2811 (s), 1524 (vs, C═N), 1485 (s), 1226 (s, thioamide), 1118 (s, N—N), 872 (m, C—S), 630 (w), 540 (w).

4.5. Crystal structure determination

Crystals of **CuL¹** (orange) and **CuL³** and **CuL⁴** (brown), suitable for X-ray diffraction studies were obtained by slow diffusion of diethyl ether into a concentrate methanolic solution of the complexes, after standing for several days, at RT. The crystals were mounted on a loop with protective oil. X-ray data were collected at 150 K on a Bruker APEX II CCD diffractometer using graphite monochromated Mo Kα radiation (0.71073°A) and operating at 50 kV and 30 mA. The X-ray data collection was monitored by the APEX2 program. All data were corrected for Lorentzian, polarization, and absorption effects using SAINT [69] and SADABS [70] programs. Structure solution and refinement were performed using direct methods with program SIR97 [71] and SHELXL97 [72] both included in the package of programs WINGX-Version 2013.3 [73]. A full-matrix least-squares refinement was used for the non-hydrogen atoms with anisotropic thermal parameters, except for disordered atoms that were refined isotropically. All hydrogen atoms were inserted in idealized positions and allowed to refine riding in the parent atom. Molecular graphics were prepared using ORTEP3 [74]. A summary of the crystal data, structure solution and refinement parameters are given in Table S1 ESI. CCDC: **CuL¹**− 147,870, **CuL³**− 1.478,471 and **CuL⁴**–1,478,472 contain the supplementary crystallographic data for this paper. These data can be obtained from The Cambridge Crystallographic Data Centre via www.ccdc.cam.ac. uk/data_request/cif.

4.6. General procedure for the synthesis and characterization of the radioactive ^{64}Cu complexes

Copper-64 was produced by the ^{64}Ni(p,n)^{64}Cu nuclear reaction in a IBA Cyclone 18/9 cyclotron and supplied as $^{64}CuCl_2$(aq) in 0.1 M HCl. Radiocopper complexes were synthesized according to previously described methods [35]. Briefly, 150 μL of $^{64}CuCl_2$ in 0.1 M HCl was

buffered with 200 μl of 3 M sodium acetate, followed by addition of 10 μL of a solution of ligand in DMSO (at 1 mg·mL^{-1}) and the reaction mixture was vortexed for 1 min. The resultant solution was left to react at RT for few seconds, and the labeling efficiency was determined by radio-HPLC using the conditions described above. t_R = 23.1 min (**CuATSM**), 24.3 min (**^{64}CuATSM**), 20.7 min (**CuL^1**), 21.2 min (**^{64}CuL^1**), 17.6 min (**CuL^2**), 18.0 min (**^{64}CuL^2**), 22.5 min (**CuL^3**), 23.0 min (**^{64}CuL^3**), 21.2 min (**CuL^4**), 21.8 min (**^{64}CuL^4**).

4.7. Lipophilicity measurements

The lipophilicity of the radiocomplexes was evaluated by the "shake-flask" method [75]. Briefly, the radioactive complexes were added to a mixture of octanol (1 mL) and 0.1 M PBS pH 7.4 (1 mL), previously saturated in each other. This mixture was vortexed and centrifuged (3000 rpm, 10 min, RT) to allow phase separation. Four aliquots of both octanol and PBS were counted in a gamma counter. The octanol-water partition coefficients were calculated by dividing the counts in the octanol phase by those in the buffer. The results expressed as log $D_{7.4}$ are presented in Table 5.

4.8. Cyclic voltammetry

Cyclic voltammetry data were obtained using a BAS C3 Cell Stand. The voltammograms were recorded at room temperature, with a scan rate of 100 mV/s, using Pt wire working and counter electrodes and a $Ag/AgNO_3$ (10^{-3} M, acetonitrile solution) reference electrode. The measurements were performed on fresh DMSO solutions with a concentration of 10^{-3} M of the analyte and 10^{-1} M of tetrabutylammonium hexafluorophoshate (n-Bu_4PF_6) as the supporting electrolyte. Ferrocene was added directly to the solution after analysis of the analyte of interest to allow the potentials normalization, in situ, relatively to the ferrocenium/ferrocene (Fc^+/Fc) couple redox potential. The $E^1_{1/2}$ ($[CuL^{\#}]^+ \rightarrow [CuL^{\#}]^0$) and $E^2_{1/2}$ ($[CuL^{\#}]^0 \rightarrow [CuL^{\#}]^-$) are reported as the mid-point between the anodic (Epa) and cathodic (Epc) peaks, $E_{1/2}$ = (Epa + Epc)/2.

4.9. DNA and albumin binding studies

Fluorescence spectra were measured on Horiba Jobin Yvon fluorescence spectrometer model FL 1065 at rRT. UV–Visible absorption (UV–Vis) spectra were recorded on a Perkin-Elmer Lambda 35 spectrophotometer at RT. Millipore water was used for the preparation of solutions and TRIS buffer (0.1 M, pH 7.4) was used in all experiments. The concentrations of HSA and CT-DNA were determined by UV–Vis absorbance using the molar absorption coefficients at 280 nm (36,850 M^{-1} cm^{-1}) and 260 nm (6600 M^{-1} cm^{-1}), respectively. HSA, CT-DNA and thiazole orange were purchased from Sigma and used as received. The stock solutions were prepared by dissolution in TRIS buffer or water (thiazole orange). The stock solutions of the complexes were prepared by dissolving/diluting them in DMSO; they were used within a few hours. The amount of organic solvent in the samples was kept below 2% (v/v).

The fluorescence experiments were done using a quartz cuvette of 1 cm path length. Bandwidths were between 5 and 7 nm in both excitation and emission. Fluorescence titrations with HSA were done in which increasing amounts of the compound's stock solution (ca. 0.6 mM) were added to the HSA solution (ca. 1.5 μM). The excitation wavelength was 295 nm and emission spectra were collected between 310 and 500 nm.

With CT-DNA, fluorescence titrations were done by adding increasing amounts of the complexes (ca. 0.3 mM) to a solution containing thiazole orange and CT-DNA (0.7:1) ([DNA] ca. 2 μM). In the competition fluorescence titrations the DNA-TO samples were excited at 509 nm and the emitted fluorescence was recorded between 520 and 700 nm.

UV–Vis absorption spectra were collected to correct the data for re-absorption and inner filter effects [56,76]. The concentrations were selected in order to have absorbance values below 0.2 at the excitation and emission wavelengths. Blank fluorescence spectra (containing everything except the fluorophore, HSA) were measured and subtracted from each sample's emission spectra.

Table 5
Octanol–water partition coefficients (log $D_{7.4}$) of $^{64}Cu^{II}$BTSC complexes.

Compound	log $D_{7.4}$ (±SD)
^{64}CuATSM	0.66 (0.13)
^{64}CuL^1	−0.23 (0.15)
^{64}CuL^2	0.02 (0.11)
^{64}CuL^3	−1.21 (0.08)
^{64}CuL^4	1.43 (0.26)

4.10. Cell culture

Human ovarian epithelial cancer A2780 (cisplatin sensitive) and A2780R (acquired cisplatin resistance) cell lines were maintained in RPMI 1640 Medium. Human cervical carcinoma cells (HeLa), breast carcinoma cells (MCF-7), melanoma cells (A375) and Human embryonic kidney cells (HEK) were grown in DMEM. Both culture mediums were supplemented with 10% heat-inactivated fetal bovine serum (FBS) and 1% penicillin/streptomycin antibiotic solution. All culture mediums and supplements were from Gibco, Invitrogen, UK. Cells were cultured in a humidified atmosphere of 95% air and 5% CO_2 at 37 °C (Heraeus, Germany).

4.11. Cytotoxicity

The potential as antitumoral agents of the BTSC-based ligands and the corresponding Cu(II) complexes was explored by the evaluation of their effects on cellular proliferation using the [1-(4.5-dimethylthiazol-2-yl)-2.5-diphenyl tetrazolium] (MTT) assay. Cells were seeded in 96-well culture plates at a density of 1.5×10^4 to 2.5×10^4 cells/well (depending of the cell line) and left to adhere overnight at 37 °C. Cells were then incubated with the Cu-complexes and respective ligands at different concentrations (0–20 μM) during 48 h at 37 °C and 5% CO_2. All tested compounds were first solubilized in DMSO (20 mM stock solution) and then diluted in culture medium for the assay, with the percentage of solvent in the culture never exceeding 0.1%. After incubation, the compounds were removed and cells washed with PBS (200 μL). The cellular viability was assessed by incubating cells with MTT (200 μL of 0.5 mg/mL solution in Modified Eagle's Medium without phenol red) during 3 h at 37 °C. The MTT solution was removed and the insoluble and blue formazan crystals formed were dissolved and homogenized with DMSO (200 μL/well). The absorbance of this colored (purple) solution was quantified by measuring the absorbance at 570 nm, using a plate spectrophotometer (Power Wave Xs; Bio-Tek). A blank solution was prepared with DMSO alone (200 μL/well). Each test was performed with at least six replicates. These results were expressed as percentage of the surviving cells in relation with the control incubated without compound. The maximum concentration of DMSO used in compounds solutions (0.1%) was not cytotoxic. IC_{50} values were determined using the Graph Pad Prism software and expressed in micromolar concentrations.

4.12. Cellular uptake

Cellular uptake assays with ^{64}Cu-complexes were performed in A2780 ovarian cancer and MCF-7 breast cancer cells seeded at a density of 0.2 million/well in a 24-well tissue culture plates. Cells were allowed to attach overnight. On the day of the experiment, cells were exposed to ^{64}Cu-complexes (about 200,000 cpm in 0.5 mL of assay medium: Modified Eagle's Medium with 25 mM HEPES and 0.2% BSA) for a period of 5 min to 4 h. Incubation was terminated by removing ^{64}Cu-complex and by washing cells twice with ice-cold PBS with 0.2% BSA. Then,

cells were lysed by 10 min incubation with 1 M NaOH at 37 °C and the activity of lysates measured. The percentage of cell-associated radioactivity was calculated and represented as a function of incubation time. Uptake studies were carried out using at least four wells for each time point.

4.13. Internalization studies

Internalization assays of the **^{64}CuATSM** and **^{64}CuL^{1}** were performed in MCF-7 human breast cancer cells seeded at a density of 0.2 million per well in 24 well-plates and allowed to attach overnight. The cells were incubated at 37 °C for a period of 5 min to 4 h with about 200,000 cpm of the radiocompound in 0.5 mL of assay medium (MEM with 25 mM HEPES and 0.2% BSA). Incubation was terminated by washing the cells with ice-cold assay medium. Cell-surface-bound radiocompound was removed by two steps of acid wash (50 mM glycine HCl/100 mM NaCl, pH 2.8) at room temperature for 4 min. The pH was neutralized with cold PBS with 0.2% BSA, and subsequently the cells were lysed by 10 min incubation with 1 M NaOH at 37 °C to determine internalized radiocompound.

4.14. Efflux studies

The cellular retention of the internalized radio-complexes was determined in A2780 and A375 cells, previously seeded in 24-well tissue culture plates, as described before for the cellular uptake assays. Cell were incubated with the ^{64}Cu-complexes for 3 h at 37 °C, washed twice with cold PBS with BSA 0.2%, and then the radioactivity released into the culture media (0.5 mL) at 37 °C was monitored during a 5 h incubation period. At different time points, the culture medium was collected and the cells were lysed with 1 M NaOH (0.5 mL). The activity in both medium (released activity) and lysates (retained activity) was counted and the percentage of cellular retention calculated and expressed as function of incubation time. The assay was carried out using at least four wells for each time point.

Acknowledgments

This work was supported by COST action CM1105 (Functional metal complexes that bind to biomolecules), Fundação para a Ciência e a Tecnologia (projects PTDC/QUI-QUI/114139/2009, EXCL/QEQ-MED/0233/2012 and UID/Multi/04349/2013; grants SFRH/BPD/29564/2006 and SFRH/BPD/80758/2011 to S. Gama and E. Palma respectively, Ciência 2008 to G. Ribeiro Morais and FCT Investigator to F. Mendes and I. Correia) and Collaborative Research Centre ChemBioSys (CRC 1127) funded by the Deutsche Forschungsgemeinschaft (DFG). The authors would also like to thank Vânia Sousa for the elemental analyses measurements and Célia Fernandes for the Mass Spectrometry analyses, which was carried out on a QITMS instrument, acquired with the support of the Programa Nacional de Reequipamento Científico (Contract REDE/1503/REM/2005-ITN) of FCT and is part of RNEM-Rede Nacional de Espectrometria de Massa.

Appendix A. Supplementary data

Supplementary data to this article can be found online at http://dx.doi.org/10.1016/j.jinorgbio.2016.11.026.

References

[1] D.X. West, J.K. Swearingen, J. Valdes-Martinez, S. Hernandez-Ortega, A.K. El-Sawaf, F. van Meurs, A. Castineiras, I. Garcia, E. Bermejo, Polyhedron 18 (1999) 2919–2929.
[2] P. Tarasconi, S. Capacchi, G. Pelosi, M. Cornia, R. Albertini, A. Bonati, P.P. Dall'Aglio, P. Lunghi, S. Pinelli, Bioorg. Med. Chem. 8 (2000) 157–162.
[3] S.E. Ghazy, M.A. Kabil, A.A. ElAsmy, Y.A. Sherief, Anal. Lett. 29 (1996) 1215–1229.
[4] A.R. Cowley, J.R. Dilworth, P.S. Donnelly, A.D. Gee, J.M. Heslop, Dalton Trans. (2004) 2404–2412.
[5] F. Cortezon-Tamarit, S. Sarpaki, D.G. Calatayud, V. Mirabello, S.I. Pascu, Chem. Rec. 16 (2016) 1380–1397.
[6] I.C. Mendes, F.B. Costa, G.M. de Lima, J.D. Ardisson, I. Garcia-Santos, A. Castineiras, H. Beraldo, Polyhedron 28 (2009) 1179–1185.
[7] J. Rivadeneira, D.A. Barrio, G. Arrambide, D. Gambino, L. Bruzzone, S.B. Etcheverry, J. Inorg. Biochem. 103 (2009) 633–642.
[8] D. Kovala-Demertzi, A. Papageorgiou, L. Papathanasis, A. Alexandratos, P. Dalezis, J.R. Miller, M.A. Demertzis, Eur. J. Med. Chem. 44 (2009) 1296–1302.
[9] M. Belicchi-Ferrari, F. Bisceglie, A. Buschini, S. Franzoni, G. Pelosi, S. Pinelli, P. Tarasconi, M. Tavone, J. Inorg. Biochem. 104 (2010) 199–206.
[10] V. Vrdoljak, I. Dilovic, M. Rubcic, S.K. Pavelic, M. Kralj, D. Matkovic-Calogovic, I. Piantanida, P. Novak, A. Rozman, M. Cindric, Eur. J. Med. Chem. 45 (2010) 38–48.
[11] U. El-Ayaan, M.M. Youssef, S. Al-Shihry, J. Mol. Struct. 936 (2009) 213–219.
[12] A.A. El-Asmy, O.A. Al-Gammal, D.A. Saad, S.E. Ghazy, J. Mol. Struct. 934 (2009) 9–22.
[13] M.-X. Li, J. Zhou, H. Zhao, C.-L. Chen, J.-P. Wang, J. Coord. Chem. 62 (2009) 1423–1429.
[14] C. Marzano, M. Pellei, F. Tisato, C. Santini, Anti Cancer Agents Med. Chem. 9 (2009) 185–211.
[15] S. Arora, S. Agarwal, S. Singhal, Int J Pharm Pharm Sci 6 (2014) 34–41.
[16] B.M. Paterson, P.S. Donnelly, Chem. Soc. Rev. 40 (2011) 3005–3018.
[17] K. A, K. S, S. J, M. D, P. DH, J. Biol. Chem. 260 (1985) 13710–13718.
[18] K.Y. Djoko, B.M. Paterson, P.S. Donnelly, A.G. McEwan, Metallomics 6 (2014) 854–863.
[19] W.K. Subczynski, W.E. Antholine, J.S. Hyde, A. Kusumi, Biochemistry 29 (1990) 7936–7945.
[20] K.A. Price, P.J. Crouch, I. Volitakis, B.M. Paterson, S. Lim, P.S. Donnelly, A.R. White, Inorg. Chem. 50 (2011) 9594–9605.
[21] D. Palanimuthu, S.V. Shinde, K. Somasundaram, A.G. Samuelson, J. Med. Chem. 56 (2013) 722–734.
[22] B.K. Bhuyan, T. Betz, Cancer Res. 28 (1968) 758–763.
[23] K.Y. Djoko, P.S. Donnelly, A.G. McEwan, Metallomics 6 (2014) 2250–2259.
[24] C.S. Cutler, H.M. Hennkens, N. Sisay, S. Huclier-Markai, S.S. Jurisson, Chem. Rev. 113 (2013) 858–883.
[25] A.L. Vavere, J.S. Lewis, Dalton Trans. (2007) 4893–4902.
[26] J.P. Holland, F.I. Aigbirhio, H.M. Betts, P.D. Bonnitcha, P. Burke, M. Christlieb, G.C. Churchill, A.R. Cowley, J.R. Dilworth, P.S. Donnelly, J.C. Green, J.M. Peach, S.R. Vasudevan, J.E. Warren, Inorg. Chem. 46 (2007) 465–485.
[27] R. Hueting, V. Kersemans, M. Tredwell, B. Cornelissen, M. Christlieb, A.D. Gee, J. Passchier, S.C. Smart, V. Gouverneur, R.J. Muschel, J.R. Dilworth, Metallomics 7 (2015) 795–804.
[28] Y. Fujibayashi, H. Taniuchi, Y. Yonekura, H. Ohtani, J. Konishi, A. Yokoyama, J. Nucl. Med. 38 (1997) 1155–1160.
[29] J.S. Lewis, D.W. McCarthy, T.J. McCarthy, Y. Fujibayashi, M.J. Welch, J. Nucl. Med. 40 (1999) 177–183.
[30] J.S. Lewis, T.L. Sharp, R. Laforest, Y. Fujibayashi, M.J. Welch, J. Nucl. Med. 42 (2001) 655–661.
[31] M. Nicoli, U. Mazzi, Proc. Proceedings of the Sixth International Symposium on Technetium in Chemistry and Nuclear Medicine, SGE, Padova, 2002 23–33.
[32] P. Burgman, J.A. O'Donoghue, J.S. Lewis, M.J. Welch, J.L. Humm, C.C. Ling, Nucl. Med. Biol. 32 (2005) 623–630.
[33] J.A. O'Donoghue, P. Zanzonico, A. Pugachev, B. Wen, P. Smith-Jones, S. Cai, E. Burnazi, R.D. Finn, P. Burgman, S. Ruan, J.S. Lewis, M.J. Welch, C.C. Ling, J.L. Humm, Int. J. Radiat. Oncol. Biol. Phys. 61 (2005) 1493–1502.
[34] R.L. Aft, J.S. Lewis, F. Zhang, J. Kim, M.J. Welch, Cancer Res. 63 (2003) 5496–5504.
[35] J.L. Dearling, J.S. Lewis, G.E. Mullen, M.J. Welch, P.J. Blower, J. Biol. Inorg. Chem. 7 (2002) 249–259.
[36] J.P. Holland, J.S. Lewis, F. Dehdashti, Q. J. Nucl. Med. Mol. Imaging 53 (2009) 193–200.
[37] J.L.J. Dearling, P.J. Blower, Chem. Commun. (1998) 2531–2532.
[38] R.I. Maurer, P.J. Blower, J.R. Dilworth, C.A. Reynolds, Y. Zheng, G.E. Mullen, J. Med. Chem. 45 (2002) 1420–1431.
[39] J.P. Holland, J.H. Giansiracusa, S.G. Bell, L.L. Wong, J.R. Dilworth, Phys. Med. Biol. 54 (2009) 2103–2119.
[40] M. Duvvuri, S. Konkar, K.H. Hong, B.S. Blagg, J.P. Krise, ACS Chem. Biol. 1 (2006) 309–315.
[41] R.A. Ndolo, Y. Luan, S. Duan, M.L. Forrest, J.P. Krise, PLoS ONE 7 (2012), e49366.
[42] H. Yu, Y. Xiao, L. Jin, J. Am. Chem. Soc. 134 (2012) 17486–17489.
[43] J. Fan, Z. Han, Y. Kang, X. Peng, Sci. Rep. 6 (2016) 19562.
[44] J. Ouyang, Q. Zang, W. Chen, L. Wang, S. Li, R.-Y. Liu, Y. Deng, Z.-Q. Liu, J. Li, L. Deng, Y.-N. Liu, Talanta 159 (2016) 255–261.
[45] A.R. Cowley, J.R. Dilworth, P.S. Donnelly, E. Labisbal, A. Sousa, J. Am. Chem. Soc. 124 (2002) 5270–5271.
[46] P.J. Blower, T.C. Castle, A.R. Cowley, J.R. Dilworth, P.S. Donnelly, E. Labisbal, F.E. Sowrey, S.J. Teat, M.J. Went, Dalton Trans. (2003) 4416–4425.
[47] D.X. West, J.S. Ives, G.A. Bain, A.E. Liberta, J. ValdesMartinez, K.H. Ebert, S. HernandezOrtega, Polyhedron 16 (1997) 1895–1905.
[48] D.X. West, A.E. Liberta, S.B. Padhye, R.C. Chikate, P.B. Sonawane, A.S. Kumbhar, R.G. Yerande, Coord. Chem. Rev. 123 (1993) 49–71.
[49] J.P. Holland, P.J. Barnard, D. Collison, J.R. Dilworth, R. Edge, J.C. Green, E.J.L. McInnes, Chemistry 14 (2008) 5890–5907.
[50] S.I. Pascu, P.A. Waghorn, B.W.C. Kennedy, R.L. Arrowsmith, S.R. Bayly, J.R. Dilworth, M. Christlieb, R.M. Tyrrell, J. Zhong, R.M. Kowalczyk, D. Collison, P.K. Aley, G.C. Churchill, F.I. Aigbirhio, Chemistry 5 (2010) 506–519.
[51] G. Wuitschik, E.M. Carreira, B. Wagner, H. Fischer, I. Parrilla, F. Schuler, M. Rogers-Evans, K. Müller, J. Med. Chem. 53 (2010) 3227–3246.
[52] C. Stefani, Z. Al-Eisawi, P.J. Jansson, D.S. Kalinowski, D.R. Richardson, J. Inorg. Biochem. 152 (2015) 20–37.

[53] B.M. Paterson, J.A. Karas, D.B. Scanlon, J.M. White, P.S. Donnelly, Inorg. Chem. 49 (2010) 1884–1893.
[54] I. Majumder, P. Chakraborty, J. Adhikary, H. Kara, E. Zangrando, A. Bauza, A. Frontera, D. Das, ChemistrySelect 1 (2016) 615–625.
[55] T.E. Kydonaki, E. Tsoukas, F. Mendes, A.G. Hatzidimitriou, A. Paulo, L.C. Papadopoulou, D. Papagiannopoulou, G. Psomas, J. Inorg. Biochem. 160 (2016) 94–105.
[56] B. Valeur, Molecular Fluorescence: Principles and Applications, Wiley-VCH Verlag, 2001 20–33.
[57] J.R. Lakowicz, Principles of Fluorescence Spectroscopy, Springer, USA, 2007.
[58] D.L. Boger, W.C. Tse, Bioorg. Med. Chem. 9 (2001) 2511–2518.
[59] C.J. Mathias, S.R. Bergmann, M.A. Green, J. Nucl. Med. 36 (1995) 1451–1455.
[60] N.E. Basken, M.A. Green, Nucl. Med. Biol. 36 (2009) 495–504.
[61] G. Buncic, J.L. Hickey, C. Schieber, J.M. White, P.J. Crouch, A.R. White, Z. Xiao, A.G. Wedd, P.S. Donnelly, Aust. J. Chem. 64 (2011) 244–252.
[62] S.R. Bayly, R.C. King, D.J. Honess, P.J. Barnard, H.M. Betts, J.P. Holland, R. Hueting, P.D. Bonnitcha, J.R. Dilworth, F.I. Aigbirhio, M. Christlieb, J. Nucl. Med. 49 (2008) 1862–1868.
[63] M. Solioz, C. Vulpe, Trends Biochem. Sci. 21 (1996) 237–241.
[64] E.D. Harris, Annu. Rev. Nutr. 20 (2000) 291–310.
[65] H. Huang, B. Yu, P. Zhang, J. Huang, Y. Chen, G. Gasser, L. Ji, H. Chao, Angew. Chem. Int. Ed. 54 (2015) 14049–14052.
[66] A.R. Cowley, J. Davis, J.R. Dilworth, P.S. Donnelly, R. Dobson, A. Nightingale, J.M. Peach, B. Shore, D. Kerr, L. Seymour, Chem. Commun. (2005) 845–847.
[67] J.P. Scovill, Phosphorus Sulfur Silicon Relat. Elem. 60 (1991) 15–19.
[68] J.P. Holland, P.J. Barnard, S.R. Bayly, H.M. Betts, G.C. Churchill, J.R. Dilworth, R. Edge, J.C. Green, R. Hueting, Eur. J. Inorg. Chem. 2008 (2008) 1985–1993.
[69] Bruker AXS Inc., Madison, Wisconsin, USA, 2005.
[70] S.G.M. Sheldrick, Madison, Wisconsin, USA, Bruker AXS Inc., 2004.
[71] A. Altomare, M.C. Burla, M. Camalli, G.L. Cascarano, C. Giacovazzo, A. Guagliardi, A.G.G. Moliterni, G. Polidori, R. Spagna, J. Appl. Crystallogr. 32 (1999) 115–119.
[72] S.G. Sheldrick, 2008.
[73] L. Farrugia, J. Appl. Crystallogr. 45 (2012) 849–854.
[74] S. Weber, J. Appl. Crystallogr. 30 (1997) 565–566.
[75] T.J. Hoffman, W.A. Volkert, D.E. Troutner, R.A. Holmes, Int. J. Appl. Radiat. Isot. 35 (1984) 223–225.
[76] A. Coutinho, M. Prieto, J. Chem. Educ. 70 (1993) 425.